

Electronic mechanism of dehydrogenation of the Mg–Ge mixture during milling under hydrogen

D.W. ZHOU^{1*}, J.S. LIU², J. ZHANG¹, Z.G. HUANG¹, P. PENG²

¹State Key Laboratory of Advanced Design and Manufacturing for Vehicle Body,
Hunan University, Changsha, 410082, China

²School of Materials Science and Engineering, Hunan University, Changsha 410082, China

The energy and electronic structure of the hydride phase are calculated by using the first-principles plane-wave pseudopotential method to explain experimental results of milling of a Mg–Ge mixture under hydrogen. The electronic mechanism of dehydrogenation of the Ge alloying system is also considered. By calculating heats of formation of MgH_2 and $(\text{MgGe})\text{H}_2$ solid solutions, it is found that the structural stability of the alloying system is reduced when a little Ge dissolves in MgH_2 . As the Ge content increases, Mg_2Ge may be formed by the reaction: $2\text{MgH}_2 + \text{Ge} \leftrightarrow \text{Mg}_2\text{Ge} + 2\text{H}_2$, at the same time, the dehydrogenating properties of the system are improved compared with that of MgH_2 , but are reduced by contrast with that of $(\text{MgGe})\text{H}_2$ solid solutions. Based on the analysis of the densities of states (DOS) of MgH_2 before and after Ge alloying, it is found that the improvement of the dehydrogenating properties of MgH_2 dissolved into a little Ge is attributed to the weakened bonding between magnesium and hydrogen caused by the interactions between Ge and Mg.

Keywords: *Mg–Ge mixture; heat of formation; electronic structure; first-principles calculation*

1. Introduction

Nowadays, many efforts have been made to develop hydrogen storage materials for non-polluting applications. Magnesium-based hydrogen storage alloys have been extensively researched, due to their high hydrogen storage capacity, light weight and low cost. However, the slow hydriding and dehydrogenating kinetics and high dissociation temperature caused by its relatively high stability limits its practical application for hydrogen storage. The reaction kinetics of Mg and hydrogen is strongly dependent on the method of synthesis and the presence of additives. Samples can be synthesized by melting, sintering or mechanical milling, each method having its own characteristics. In particular, ball milling produces special microstructures, metastable phase, modified surfaces, defects, etc., which generally improve the hydriding

*Corresponding author, e-mail: ZDWe_mail@yahoo.com.cn

–dehydrogenating process [1, 2]. Recent experimental investigations [1, 3–10] have shown that the mechanical alloying of MgH_2 and 3d elements such as Ni, Co, Mn, Cu, Ti, Fe, V, non-3d elements – Ge, Nb, intermetallic compounds – LaNi_5 , FeTi , $\text{ZrFe}_{1.4}\text{Cr}_{0.6}$, effectively improves the hydriding and dehydrogenating kinetics of MgH_2 at high temperature. In this work, at first, experimental results of milling of Mg–Ge mixture under hydrogen as described by Gennari et al. [5], are introduced, then, the energy and electronic structure of the hydride phases are calculated by using the first-principles plane-wave pseudopotential method to explain the experimental results from Gennari et al., Moreover, the dehydrogenating properties of milling the Mg–Ge mixture under hydrogen and the electronic mechanism of the Ge alloying system are analyzed and discussed.

2. Experimental results

Mg was initially milled for up to 100 h under a hydrogen atmosphere, and sequential XRD patterns were obtained after various milling times with Ge addition, which is the same method as that used by Gennari et al. [5]. It can be found that the tetragonal $\beta\text{-MgH}_2$ and orthorhombic $\gamma\text{-MgH}_2$ were synthesized by RMA of Mg after 75 h, and the broadening of the $\beta\text{-MgH}_2$ and $\gamma\text{-MgH}_2$ peaks was observed for a milling time of between 75 to 100 h.

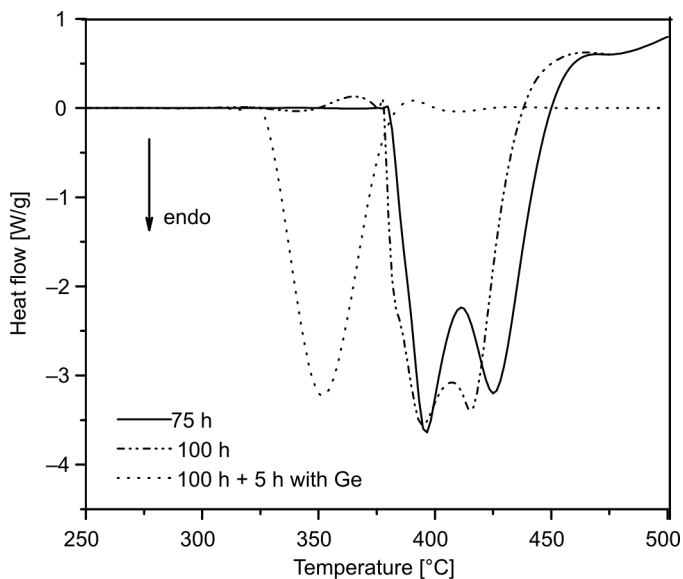


Fig. 1. DSC curves from Mg milled with and without Ge under hydrogen atmosphere for different milling time

Figure 1 shows the DSC curves of Mg initially milled for up to 100 h under a hydrogen atmosphere. For 75 and 100 h of milling, the curve shows a double endother-

mic peak located around 400 °C. When Ge (5 at. %) was added to Mg after 100 h of RMA, significant structural modifications were observed by Gennari et al. [5]. The XRD pattern shows that after 5 h of milling, compound Mg_2Ge appears. From the intensity of the peaks, the amount of Mg_2Ge increases with the milling time, whereas the amount of Ge decreases. In addition, the DSC curve (Fig. 1) shows a sharp endothermic peak at 355 °C. Thus, Ge addition decreases the temperature for hydrogen desorption at about 50 °C compared with pure Mg after 100 h of RMA.

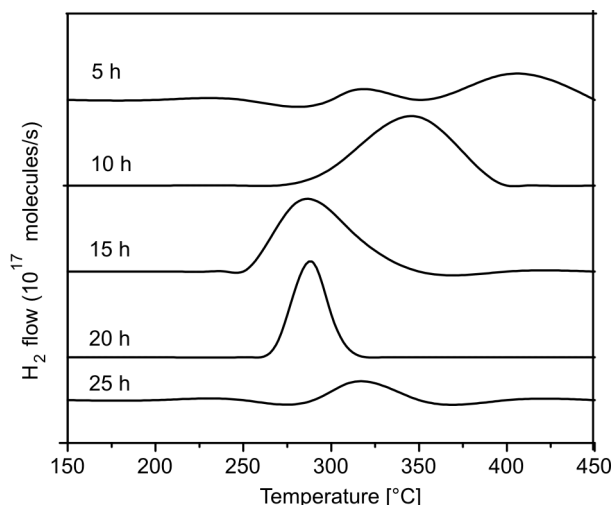


Fig. 2. TDS hydrogen spectra of Mg–Ge after RMA for different milling times

The Mg–Ge mixture was milled under a hydrogen atmosphere for various times. As the milling time increases, the intensity of the peaks corresponding to Mg and Ge decreases. The Mg_2Ge and $\beta\text{-MgH}_2$ hydride appear after 5 h of milling. The intensity of the peaks associated with Mg_2Ge grows with the milling time, whereas the peaks corresponding to the hydride initially increase and then decrease. The TDS spectra that describe the entire evolution of the hydrogen desorption kinetics for between 5 and 25 h of milling are shown in Fig. 2. For 5 to 15 h of milling, desorption peaks shift towards lower temperatures. In this range of milling time, the amount of hydride grows and desorption improves as a consequence of better Ge and MgH_2 intermixing. After 15 h or more, such as after 20 h, the effect reverses which can be seen in Fig. 2. Desorption begins at higher temperatures. This is a consequence of the consumption of Ge to form Mg_2Ge , as can be seen from the XRD patterns given by Gennari et al. [5]. After 25 h of milling, the amount of hydride that remains on the sample is hardly detected.

The above experimental results from Gennari et al. [5] show that Ge has an important effect on the hydrogen desorption process. This effect is enhanced with the milling time, probably due to a better Ge intermixing or because a little Ge is dissolved in

the magnesium hydride. As the Ge content increases, Mg_2Ge may be formed by the reaction:



at the same time the dehydrogenating properties of the system are improved compared with those of MgH_2 , but reduced by contrast with those of $(\text{MgGe})\text{H}_2$ solid solutions. However, more effort is needed to explain the experimental results shown in Figs. 1 and 2. Moreover, electronic mechanism on the dehydrogenating properties of Ge alloying magnesium hydride is also worth studying.

3. Method and models of computation

The Cambridge Serial Total Energy Package (CASTEP) [11], a first-principles plane-wave pseudopotentials method, based on density functional theory, was used in this work. The CASTEP uses a plane-wave basis set for the expansion of single particle Kohn–Sham wave functions, and pseudopotentials to describe the computationally expensive electron–ion interaction, in which the exchange–correlation energy with the generalized gradient approximation (GGA) of Perdew was used for all elements in our models by adopting the Perdew–Burke–Ernzerhof parameters [12]. The ultrasoft pseudopotential, represented in the reciprocal space, was used [13]. In the present calculations, the cutoff energy of atomic wave functions (PWs) E_{cut} , was set at 310 eV. Sampling of the irreducible wedge of the Brillouin zone was performed with a regular Monkhorst–Pack grid of special k -points, in a $6 \times 6 \times 6$ configuration. A finite basis set correction and the Pulay scheme of density mixing [14, 15] were applied for the evaluation of energy and stress. All atomic positions in our model have been relaxed according to the total energy and force, using the BFGS scheme [16], based on the cell optimization criterion (RMs force of $0.05 \text{ e V}/\text{\AA}$, stress of 0.1 GPa , and displacement of 0.002 \AA). The calculation of the total energy and electronic structure are followed by the cell optimization with the SCF tolerance of $2.0 \times 10^{-6} \text{ eV}$.

In this work, the unit cell, super cell model of MgH_2 and the crystal model of Mg_2Ge are used for studying the dehydrogenating properties of milling the Mg–Ge mixture under a hydrogen atmosphere and for studying the electronic mechanism of Ge alloying magnesium hydride. The lattice parameters of MgH_2 with a tetragonal symmetry ($P4_2/mnm$, Group No.136) are $a = 4.501 \text{ \AA}$ and $c = 3.010 \text{ \AA}$. The positions of atoms are $+2\text{Mg}(0,0,0)$ and $+4\text{H}(0.304,0.304,0)$, respectively [17], as shown Fig. 3a. Two hypothesised super cells with 3 and 5 times in c axis of MgH_2 unit cell are shown in Figs. 3b, and 3c, respectively. When a little Ge is dissolved in MgH_2 , it is thought that $(\text{MgGe})\text{H}_2$ solid solutions are formed. As far as the solution concentration of Ge in MgH_2 is concerned, one Mg atom in threefold unit cell (Fig. 3b) or fivefold unit cell (Fig. 3c) is replaced by Ge atoms. Therefore, the corresponding super cell with Ge additions is $(\text{Mg}_3\text{Ge})\text{H}_{12}$ with 8.33 at. % of Ge or $(\text{Mg}_5\text{Ge})\text{H}_{20}$ with 5.0 at. % of Ge.

Two Mg atoms in threefold unit cell (Fig. 3b) or fivefold unit cell (Fig. 3c) are replaced by Ge atoms. Hence, the corresponding super cells are $(\text{Mg}_4\text{Ge}_2)\text{H}_{12}$ with 16.67 at. % of Ge or $(\text{Mg}_8\text{Ge}_2)\text{H}_{20}$ with 10.0 at. % of Ge.

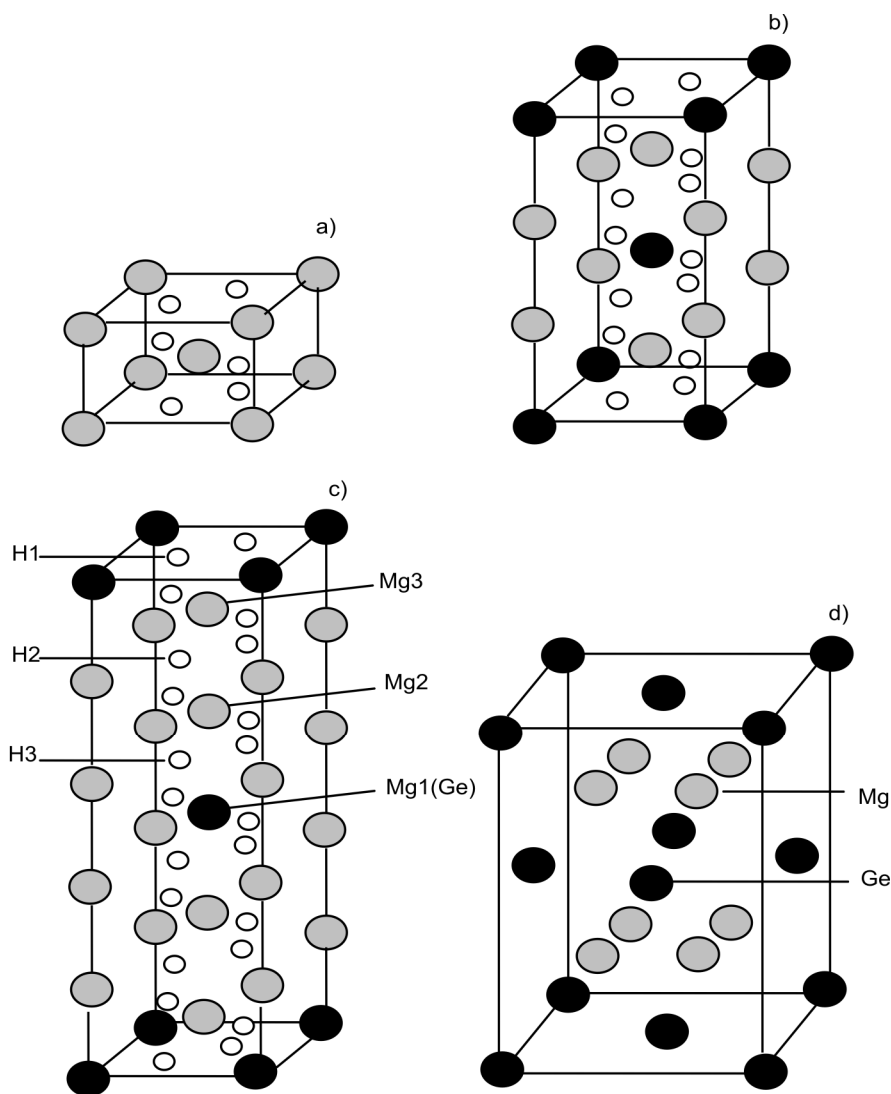


Fig. 3. Model of a unit cell of MgH_2 phase (a), threefold (b), and fivefold unit cells (c) of MgH_2 phase, cell of Mg_2Ge (d), where the nonequivalent atoms are denoted by the numbers 1–3

The lattice parameters of Mg_2Ge with CaF_2 -type structure ($Fm\bar{3}m$, group No. 225) are $a = b = c = 6.370 \text{ \AA}$. The positions of atoms are $+8\text{Mg} (0.25, 0.25, 0.25)$ and $+4\text{Ge} (0, 0, 0)$, respectively [18] (Fig. 3d). Hence, the chemical formula of Mg_2Ge crystal cell can be expressed as Mg_8Ge_4 . Here, it must be pointed out that when the Ge

content of the (MgGe)H₂ solid solution is 20.0 at. %, the following reaction may proceed:



4. Results from first-principles calculations

4.1. Dehydrogenating properties

Thermodynamic aspects of formation/decomposition of magnesium hydride can be described by pressure–composition isotherms at a given temperature. The overall reaction of hydride formation consists of three steps. Firstly, the host metal dissolves some H atoms to form a solid solution, i.e., α -Mg(H) phase. Secondly, under increasing pressure of hydrogen or oncentration of H in the host metal, the interactions between H atoms locally strengthen and lead to nucleation and growth of the tetragonal β -MgH₂ phase. While the two phases of α and β coexist, the isotherms appear as a flat plateau, their lengths show how many H₂ can be stored with small pressure variations. This plateau or equilibrium pressure depends strongly on temperature and is related to the changes of enthalpy (ΔH) and of entropy (ΔS). Finally, the concentration of H in the host metal shows no further change if the hydrogen pressure continues to increase. The reaction of hydride decomposition is opposite to hydride formation, but occurs in time retardation compared with hydride formation. During the second step, it is often related to the equilibrium hydrogen pressure through the van't Hoff equation [19]:

$$\ln\left(\frac{P}{P_0}\right) = \frac{\Delta H}{RT} - \frac{\Delta S}{R} \quad (1)$$

where P is a flat plateau pressure for decomposition, P° is the standard pressure (0.1 MPa), ΔH is the heat of formation, ΔS is the entropy change, T is temperature and R is the gas constant. The entropy change in Eq. (1) is dominated by the entropy loss of gaseous hydrogen, roughly 130.8 J/mol [19] for the MgH₂ under consideration. Hence, Eq. (1) can be expressed as

$$\frac{\partial\left(\ln\frac{P}{P^\circ}\right)}{\partial\left(\frac{1}{T}\right)} = \frac{\Delta H}{R} \quad (2)$$

From Equation (2), it can be found that ΔH of magnesium hydride determines the flat plateau pressure of decomposition of magnesium hydride at a given temperature. The smaller the heat of formation, the lower the pressure is, which indicates the enhanced dehydrogenating properties of magnesium hydride [20, 21]. Hence, one need

only concentrate on the heat of formation in order to understand the dehydrogenating properties of magnesium hydride.

4.2. Heat of formation

The lattice constants of Mg_2Ge , MgH_2 , Ge and hcp-Mg are estimated from the minimized total energy (Table 1). It can be found that the lattice parameter a of Mg_2Ge is 6.370\AA , which is close to the experimental values (6.3849\AA) in Ref. [18], and also in agreement with the calculated results (6.309\AA [18], 6.12\AA [22]). At the same time, we can calculate that the lattice parameters a and c of MgH_2 are 4.533\AA and 3.022\AA , respectively, which are close to the experimental values of $a = 4.501\text{\AA}$ and $c = 3.010\text{\AA}$ in Ref. [17] and are also in agreement with the results ($a = 4.535\text{\AA}$ and $c = 3.023\text{\AA}$) calculated by Song et al. [20]. Moreover, the calculated lattice parameters a and c of hcp-Mg are 3.152\AA and 5.435\AA , respectively, which are close to the experimental values of $a = 3.211\text{\AA}$ and $c = 5.215\text{\AA}$ in Ref. [23]. Hence it can be concluded that the computational methods used in the present work are indeed effective.

Table 1. Equilibrium lattice constants and total energies of the crystal and super cell model

Material	Lattice parameter [\AA]		Total energy of the crystal cell [eV]	Total energy of the primitive cell [eV]
	a	c		
Mg	3.152	5.435	−977.8677	−1010.0786
Ge	5.658	—	−109.2592	
MgH_2	4.533	3.022	−2020.1572	
	4.533	9.069	−6060.4722	
MgH_2	4.533	15.104	−10100.7856	
$(\text{Mg}_5\text{Ge})\text{H}_{12}$	4.556	9.218	−5189.0300	
$(\text{Mg}_4\text{Ge}_2)\text{H}_{12}$	4.545	9.371	−4317.8333	
$(\text{Mg}_9\text{Ge})\text{H}_{20}$	4.543	15.282	−9229.3451	
$(\text{Mg}_8\text{Ge}_2)\text{H}_{20}$	4.566	15.378	−8357.9166	
Mg_8Ge_4	6.370	—	−8263.2466	

The heat of formation of MgH_2 can be calculated from [20]

$$\Delta H_{\text{MgH}_2} = E_{\text{tot}}(\text{MgH}_2) - E_{\text{tot}}(\text{Mg}) - E_{\text{tot}}(\text{H}_2) \quad (3)$$

where $E_{\text{tot}}(\text{MgH}_2)$ is the energy of the primitive cell of MgH_2 , $E_{\text{tot}}(\text{Mg})$ is a single atomic energy of hcp-Mg in the solid state, and $E_{\text{tot}}(\text{H}_2)$ is the total energy of the hydrogen molecule. The calculation energies of Mg atoms are also listed in Table 1 using the same code as for the primitive cell model. The total energy of the hydrogen molecule was calculated as -2.320Ry (ca. -31.5652 eV) [24], using the von Barth-Hedin exchange correlation potential. The $\Delta H(\text{MgH}_2)$ value ($-62.30\text{ kJ}/(\text{mol H}_2)$) in

this work is slightly higher than -73.5 kJ/(mol H_2) deduced from the thermodynamic data at $T \approx 673$ K and reported by Bogdanović et al. [24]. Taking into account that the temperature of computation is different from that of the experiment, the present results of computation should be suitable.

The heat of formation of $(MgGe)H_2$ solid solution is calculated from [25, 26]

$$\Delta H_1 = \frac{1}{6} [E_{tot}(Mg_{6-x}Ge_xH_{12}) - (6-x)E_{tot}(Mg) - xE_{tot}(Ge) - 6E_{tot}(H_2)] \quad (4)$$

$$\Delta H_2 = \frac{1}{10} [E_{tot}(Mg_{10-x}Ge_xH_{20}) - (10-x)E_{tot}(Mg) - xE_{tot}(Ge) - 10E_{tot}(H_2)] \quad (5)$$

Here $E_{tot}(Mg_{6-x}Ge_xH_{12})$ and $E_{tot}(Mg_{10-x}Ge_xH_{20})$ are the energies of three or five MgH_2 unit cells with Ge addition, respectively. $E_{tot}(Ge)$ is the energy of per Ge atom, X denotes the number of atoms replaced by Ge. The total energies of the $(Mg_5Ge)H_{12}$, $(Mg_9Ge)H_{20}$, $(Mg_4Ge_2)H_{12}$, $(Mg_8Ge_2)H_{20}$ super cell are calculated and the results are also listed in Table 1. The heat of formation of $(MgGe)H_2$ solid solutions, calculated from Eq. (4) and Eq. (5), are shown in Fig. 4. When the Ge content changes from 0 to 10.0 at. %, the heat of formation of the system is negative but the absolute value gradually decreases compared with that of MgH_2 . However, when the Ge content is above 10.0 at. %, its value is positive, which means the system is unstable.

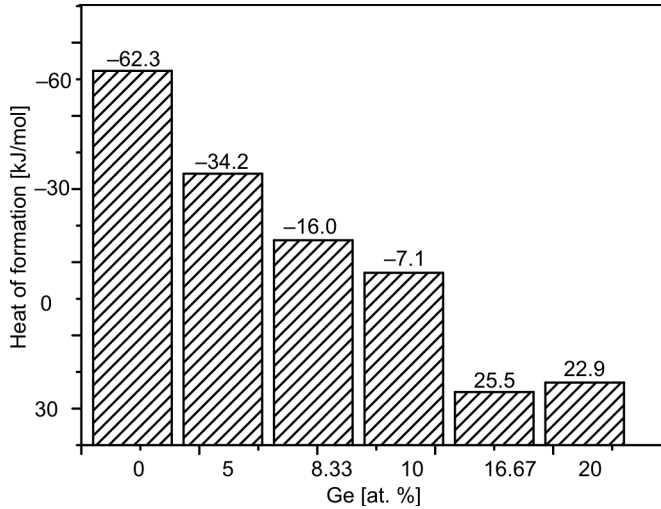
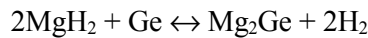


Fig. 4. Heat of formation of MgH_2 and $(MgGe)H_2$

The change of the energy from the reaction of



is calculated from [23]

$$\Delta H_3 = \frac{1}{2} [E_{\text{tot}}(\text{Mg}_2\text{Ge}) + 2E_{\text{tot}}(\text{H}_2) - 2E_{\text{tot}}(\text{MgH}_2) - E_{\text{tot}}(\text{Ge})] \quad (6)$$

Here $E_{\text{tot}}(\text{Mg}_2\text{Ge})$ is the energy of the primitive cell of Mg_2Ge . The calculated energy of Mg_2Ge is listed in Table 1. Its value is 22.9 (kJ/mol H_2) from Eq. (6), which means that the amount of released heat during the reaction



is smaller than 25.5 kJ/mol H_2 of $(\text{Mg}_4\text{Ge}_2)\text{H}_{12}$ solid solutions containing 16.7 % Ge. Hence, as the Ge content increases, Mg_2Ge may be formed in the above reaction.

The parameter $\Delta E_r(\text{Mg}_2\text{Ge})$ is used to estimate the influence of Mg_2Ge on the dehydrogenating properties of MgH_2 . It is calculated from [20]:

$$\Delta E_r(\text{Mg}_2\text{Ge}) = E_{\text{tot}}(\text{Mg}_8\text{Ge}_2\text{H}_{20}) - 10E_{\text{tot}}(\text{MgH}_2) - 2E_{\text{tot}}(\text{Mg}_2\text{Ge}) + 6E_{\text{tot}}(\text{Mg}) \quad (7)$$

Here the calculated value of $\Delta E_r(\text{Mg}_2\text{Ge})$ is 69.3 kJ/mol H_2 .

4.3. Electronic structure

Analysis of the total and partial density of states (DOS) of three- and fivefold Ge alloying MgH_2 unit cells is performed to understand the electronic mechanisms of the change of structural stability. The total and partial DOSs of $\text{Mg}_{10}\text{H}_{20}$, $(\text{Mg}_9\text{Ge})\text{H}_{20}$ and $(\text{Mg}_8\text{Ge}_2)\text{H}_{20}$ are plotted in Figs. 5a–c, respectively. The signs of Mg, Ge, H atoms are as shown in Fig. 3c. Figure. 5a shows the DOS of MgH_2 system without Ge addition. It is found that the main bonding peaks lie in the energy region between the Fermi energy (E_F) and -7.0 eV. The bonding peak between E_F and -3.0 eV mainly originates from the contribution of valence electrons of H(s), Mg(p) and a few Mg(s) orbitals. The bonding peak between -4.0 eV and -3.0 eV corresponds to the interaction between H(s) and Mg(s) as well as a few Mg(p) electrons. The bonding peak between -7.0 eV and -4.0 eV results from the bonding of valence electrons of H(s) and Mg(s). For Ge alloying the MgH_2 unit cell, a distinct difference in DOS between Fig. 5b and Fig. 5c can be seen:

- Compared with the MgH_2 super cell without Ge addition, the gap between the -2.0 eV and -1.0 eV in the MgH_2 super cell disappears.
- The bonding electron numbers between -2.0 eV and 2.0 eV result mainly from the presence of Ge(s) orbits. For the $(\text{Mg}_9\text{Ge})\text{H}_{20}$ model, the bonding peaks increase the contribution of a few Mg2(p) and H3(s). For the $(\text{Mg}_8\text{Ge}_2)\text{H}_{20}$ model, not including the contribution of Mg2(p) and H3(s), the bonding peaks increase the contribution of valence electrons of a few Mg3(p), H1(s) and H2(s) orbitals.
- For the $(\text{Mg}_9\text{Ge})\text{H}_{20}$ model, compared with the MgH_2 super cell without Ge addition, the heights of the bonding peaks of H3 significantly increase between -9.0 eV and

–11.0eV, and the bonding peaks increase the contribution of Ge(s) orbitals. For the $(\text{Mg}_8\text{Ge}_2)\text{H}_{20}$ model, not including the contribution of valence electrons of Ge(s), the height of the bonding peaks of H3 and H1 both significantly increase in the same region. In addition, the height of the bonding peaks of Mg(s), Mg(p) and H(s) decrease near E_F . Hence, when a little Ge dissolves in magnesium hydride, the weakened bonding between magnesium and hydrogen is caused by the interactions between Ge and Mg [20].

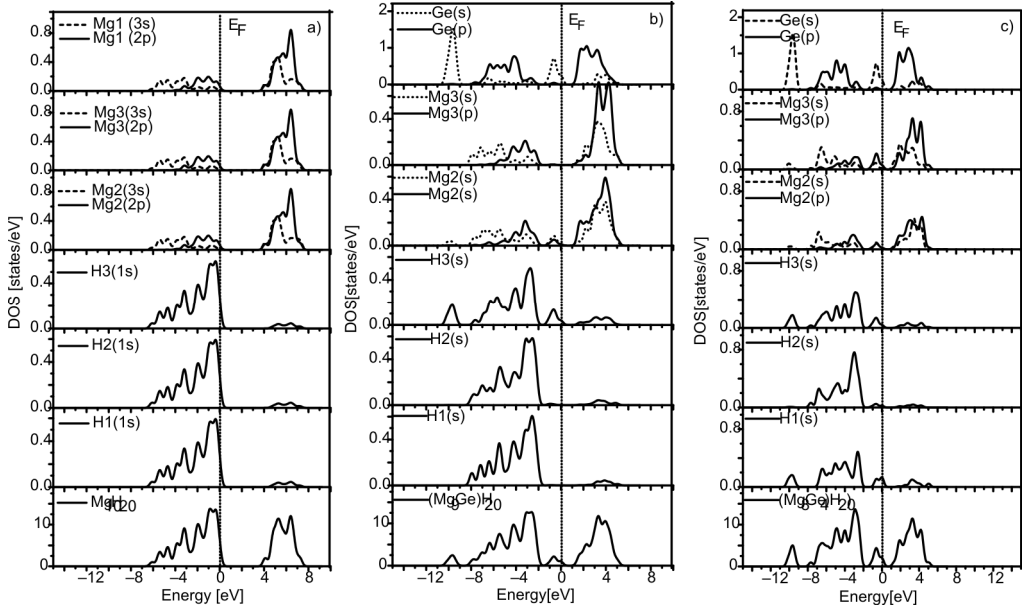


Fig. 5. Total and partial densities of states of: a) $\text{Mg}_{10}\text{H}_{20}$, b) $(\text{Mg}_9\text{Ge})\text{H}_{20}$, c) $(\text{Mg}_8\text{Ge}_2)\text{H}_{20}$

4.4. Influence of Ge on dehydrogenating properties of MgH_2

In Section 4.2, it can be found that when the Ge content changes from 0 to 10.0 at. %, the heat of formation of the Ge alloying system is negative but the absolute value gradually decreases compared with that of MgH_2 . However, in case the Ge content exceeds 10.0 at. %, its value is positive because the heat of formation of magnesium hydride determines the flat plateau pressure of magnesium hydride decomposition at a given temperature T . The smaller the heat of formation, the lower the pressure is. Hence, for Mg–Ge powder mixtures, with increasing milling time, a small amount of Ge are dissolved into MgH_2 to form $(\text{MgGe})\text{H}_2$ solid solutions. Hence, for Mg–Ge powder mixtures, as the milling time increases, a small amount of Ge is dissolved in the MgH_2 to form $(\text{MgGe})\text{H}_2$ solid solutions. As the concentration of the Ge solution in the MgH_2 lattice increases, the dehydrogenating properties of the system are improved compared with the system without Ge addition, which is in good agree-

ment with the results shown in Fig.1 and Fig.2 from the analysis of Gennari et al. [5]. The value 22.9 (kJ/mol H₂) from Eq. (6) is smaller than 25.5 (kJ/mol H₂) for (Mg₄Ge₂)H₁₂ solid solutions. Hence, as the Ge content increases, Mg₂Ge may be formed by the reaction: $2\text{MgH}_2 + \text{Ge} \leftrightarrow \text{Mg}_2\text{Ge} + 2\text{H}_2$ (Fig. 4). As the Ge content increases, the dehydrogenating properties of the system are improved compared with those with the system without Ge addition but not as good as those of (MgGe)H₂ solid solutions, which is in good agreement with the results of milling for 20 h, as shown in Fig. 2 from the analysis of Gennari et al. [5]. Moreover, the calculated value for $\Delta E_r(\text{Mg}_2\text{Ge})$ from Eq. (7) is 69.3 kJ/mol H₂. Since the modified MgH₂ phase is still the major phase in the coexistence mixtures of two types of hydrides: $\beta\text{-MgH}_2$ and Mg₂Ge [5], which indicates that Mg₂Ge phase acts as a catalyst, it can therefore reduce the structural stability of MgH₂ and further improve its dehydrogenating properties, which is in good agreement with the results from the analysis of Gennari et al. [5] (Fig. 3).

5. Conclusions

Based on the experimental results of milling the Mg–Ge mixture under a hydrogen atmosphere, as obtained by Gennari et al., the energy and electronic structure of the hydride phase are calculated by using a first-principles plane-wave pseudopotential method based on the density functional theory. The main conclusions are summarized as follows: (1) when a little Ge dissolves in magnesium hydride, the structural stability of the alloying system is reduced compared with that of MgH₂; (2) as the Ge content increases, Mg₂Ge may be formed in the reaction: $2\text{MgH}_2 + \text{Ge} \leftrightarrow \text{Mg}_2\text{Ge} + 2\text{H}_2$, while at the same time the dehydrogenating properties of the system are improved compared with that of MgH₂ but are reduced by contrast with that of (MgGe)H₂ solid solutions; (3) the improvement in the dehydrogenating properties of MgH₂ in which a small quantity of Ge is dissolved, results in weakened bonding between magnesium and hydrogen caused by the interactions between Ge and Mg.

Acknowledgements

The work was supported by the Hunan University basic scientific research and operational costs of central colleges (No. 531107040038).

References

- [1] LIANG G., HUOT J., BOILY S., SCHULZ R., J. Alloys Compd., 305 (2000), 239.
- [2] SELVAM P., MOHAPATRA S.K., SONAVANE S.U., JAYARAM R.V., Appl. Catal. B Environ., 49 (2004), 251.
- [3] SHANG C.X., BOUOUDINA M., SONG Y., GUO Z.X., Int J. Hydr. En., 29(2004), 73.
- [4] AKIBA E., HAYAKAWA H., HUOT J., J. Alloys Compd, 248 (1997), 164.
- [5] GENNARI F.C., CASTRO F.J., URRETAVIZCAYA G., MEYER G., J. Alloys Compd, 334 (2002), 277.

- [6] TESSIER J.P., PALAU P., HUOT J., SCHULZ R., GUAY D., J. Alloys Compd, 376 (2004), 180.
- [7] LIANG G., HUOT J., BOILY S., VAN N.A., SCHULZ R., J. Alloys Compd., 292 (1999), 247.
- [8] LIANG G., HUOT J., BOILY S., VAN N.A., SCHULZ R., J. Alloys Compd., 297 (2000), 261.
- [9] MANDAL P., DUTTA K., RAMAKRISHNA K., SAPRU K., SRIVASTAVA O.N., J. Alloys Compd., 184 (1992), 1.
- [10] WANG P., WANG A.M., DING B.Z., HU Z.Q., J. Alloys Compd, 334 (2002), 243.
- [11] LINDAN P.L.D., SEGALL M.D., PROBERT M.J., PICKARD C.J., HASNIP P.J., CLARK S.J., PAYNE M.C., J. Phys: Cond. Matter, 14 (2002), 2717.
- [12] MARLO M., MILMAN V., Phys. Rev. B, 62 (2000), 2899.
- [13] VANDERBILT D., Phys. Rev. B, 41 (1990), 7892.
- [14] HAMMER B., HANSEN L.B., NORKOV J.K., Phys. Rev. B, 59 (1999), 7413.
- [15] FRANCIS G.P., PAYNE M.C., J. Phys. Cond. Matter, 2 (1990), 4395.
- [16] MONKHORST H.J., PACK J.D., Phys. Rev. B, 13 (1976), 5188.
- [17] BORTZ M., BERTHEVILLE B., BÖTTGER G., YVON K., J. Alloys Compd., 287 (1999), L4.
- [18] GROSCH G.H., RANGE K.J., J. Alloys Compd., 235 (1996), 250.
- [19] NAKAMURA H., NGUYEN M.D., PETTIFOR D.G., J. Alloys Compd., 281 (1998), 81.
- [20] SONG Y., GUO Z.X., YANG R., Phys. Rev. B, 69 (2004), 094205.
- [21] NAMBU T., EZAKI H., YUKAWA H., MORINAGA M., J. Alloys Compd., 293–295 (1999), 213.
- [22] CORKILL J. L., COHEN M.L., Phys. Rev. B, 48 (1993), 17138.
- [23] HUOT J., BOILY S., AKIBA E., SCHULZ R., J. Alloys Compd., 280 (1998), 306.
- [24] BOGDANOVIC B., BOHMHAMMELK., CHRIST B., REISER A., SCHLICHTE K., VEHLER R., WOLF U., J. Alloys Compd., 282 (1999), 84.
- [25] MEDVEDEVA M.I., GORNOSTYREV Y.N., NOVIKOV D.L., MRYASOV O.N., FREEMAN A.J., Acta Mater., 46 (1998), 3433.
- [26] SAHU B.R., Mater. Sci. Eng. B, 49, (1997), 74.

Received 4 April 2008

Revised 24 November 2009